Electronic Supplementary Material (ESI) for Journal of Materials Chemistry A.

Supporting informations

Elastic Ag Anchored N-doped Graphene/Carbon Foam for the Selective Electrochemical Reduction of Carbon Dioxide to Ethanol

Kuilin Lv, †,[a] Yanchen Fan, †, [b] Ying Zhu,[a] Yi Yuan,[a] Jinrong Wang,[a] Ying Zhu*[a, c] and Qianfan Zhang*[b]

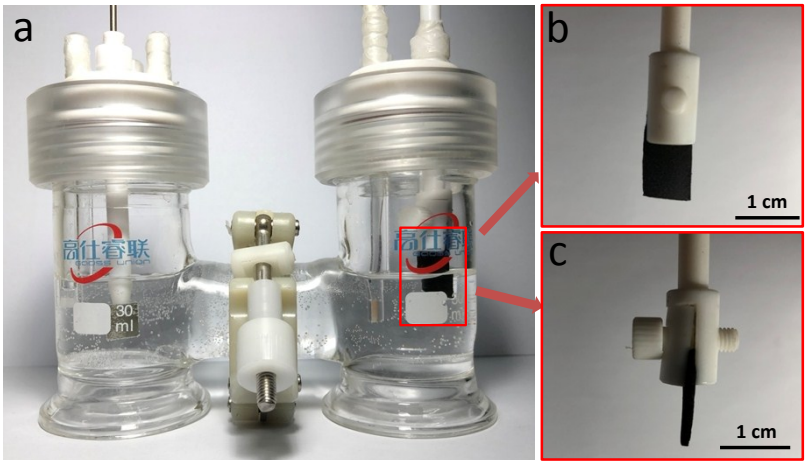

Figure S1. (a) The photograph of electrolytic cell. (b, c) Ag-G-NCF foam is fixed on the alligator clip as the working electrode.

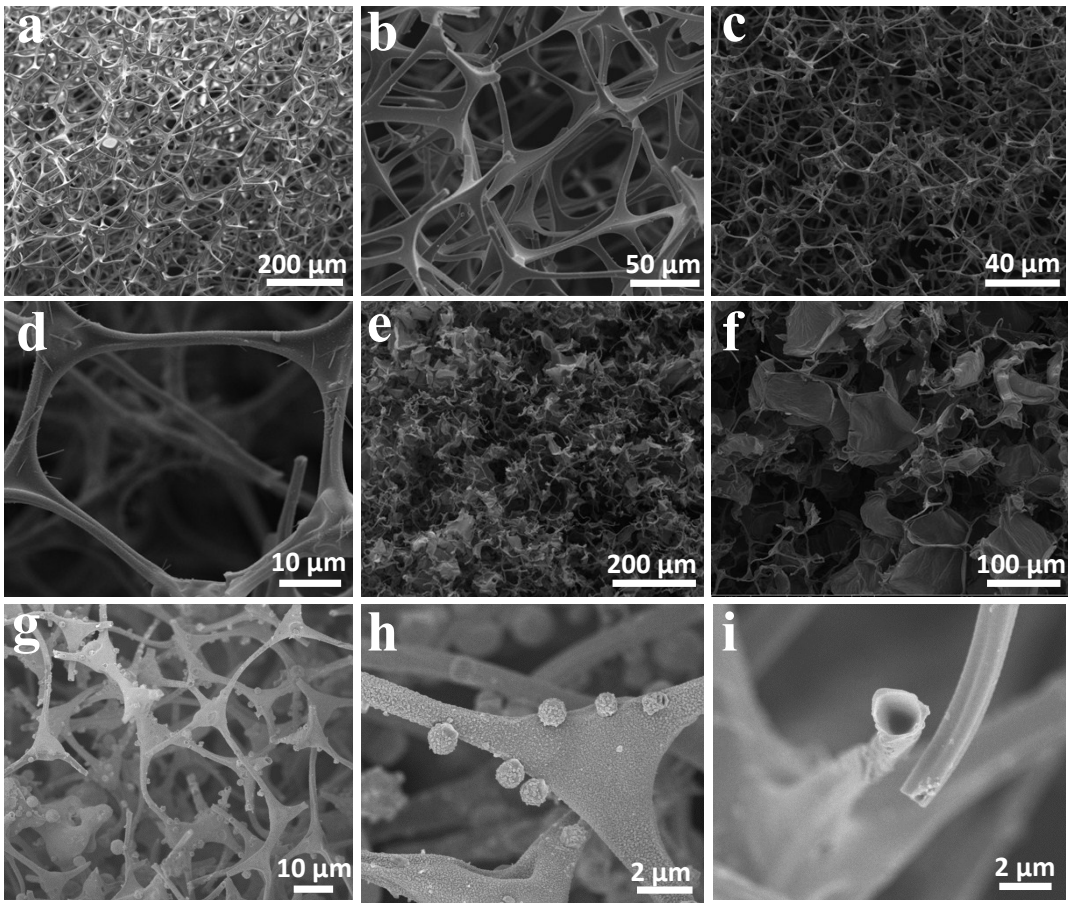

Figure S2. (a, b) SEM images of MF. (c, d) SEM images of NCF. (e, f) SEM images of G-NCF. (g, h) SEM images of Ag-NCF. (i) SEM image of NCF, presenting the hollow structure of the framework of NCF.

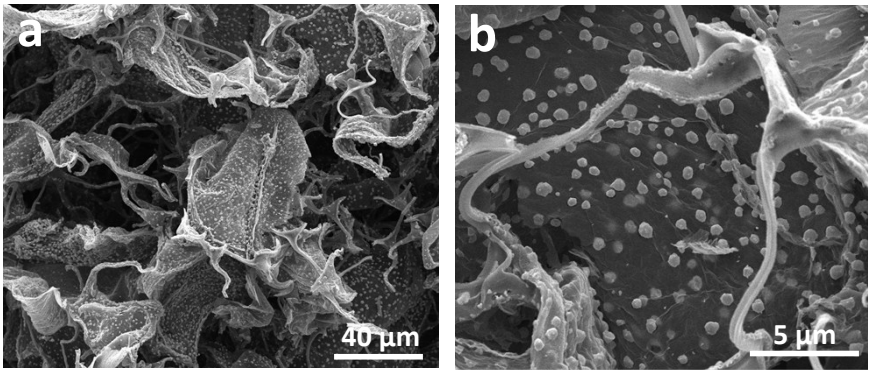

Figure S3. (a, b) SEM images of Ag-G-NCF.

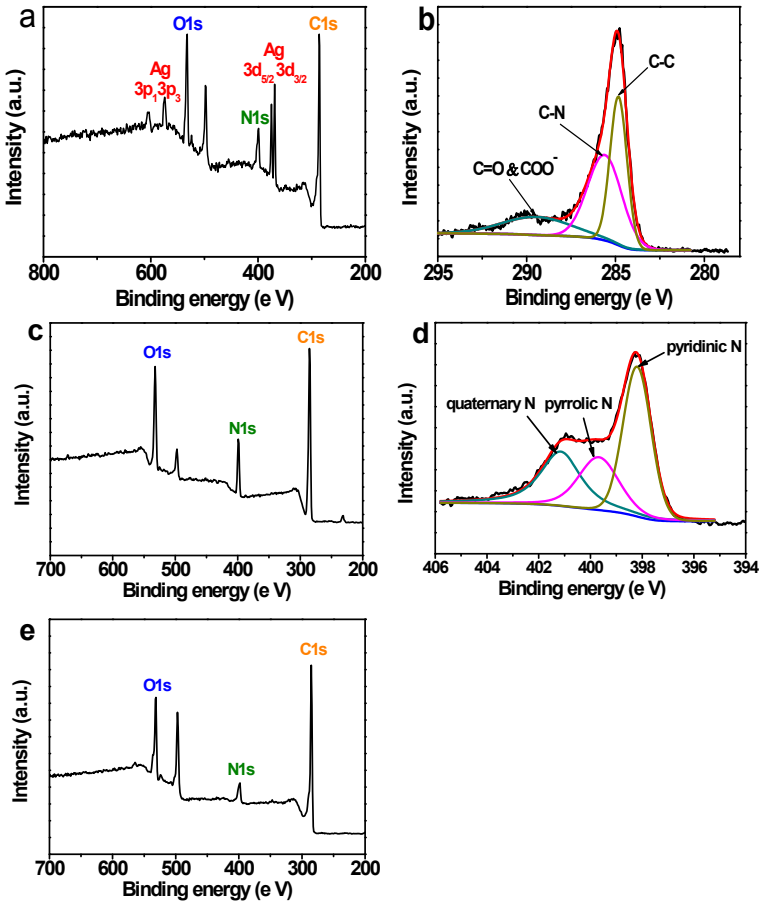

Figure S4. (a) XPS survey spectrum of Ag-G-NCF. (b) High resolution C 1s XPS spectrum of Ag-G-NCF. (c) XPS survey spectrum of NCF. (d) High resolution N 1s XPS spectrum of NCF. (e) XPS survey spectrum of MF.

Table S1. The element contents on MF, NCF, and Ag-G-NCF by XPS spectrum

	C (at.%)	O (at.%)	Ag (at.%)	N (at.%)	Graphitic N (at.%)	Pyrrolic N (at.%)	Pyridinic N (at.%)
MF	75.7	16.2	—	8.1	—	—	—
NCF	81.9	8.9	—	9.2	2.2	2.3	4.7
Ag-G-NCF	80.4	9.4	1.3	8.9	2.1	2.3	4.5

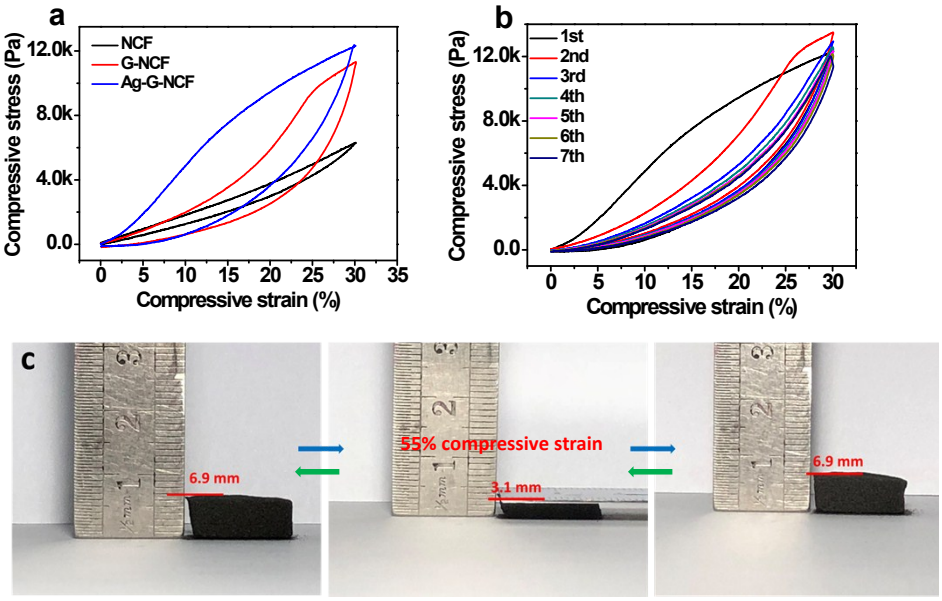

Figure S5. (a) Representative compression test curves of NCF, G-NCF and Ag-G-NCF. (b) Loading and unloading compressive stress-strain curves of Ag-G-NCF over 7 cycles. (The second cycle is recorded with 20 min rest after the first test). (c) Reversible elastic deformation of the Ag-G-NCF sample under strain.

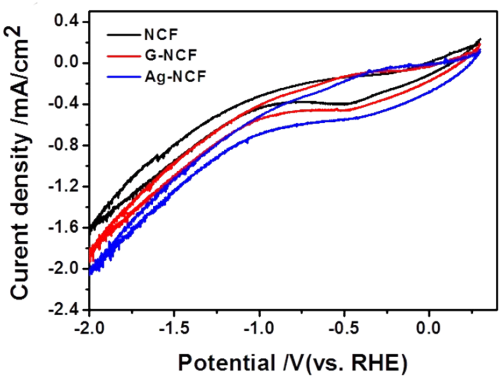

Figure S6. CV curves in potential range of 0.5 V to -1.8 V (vs RHE) at a sweep rate of 0.02 V s^{-1} on NCF (black), G-NCF (red) and Ag-NCF (blue) under CO_2 atmosphere.

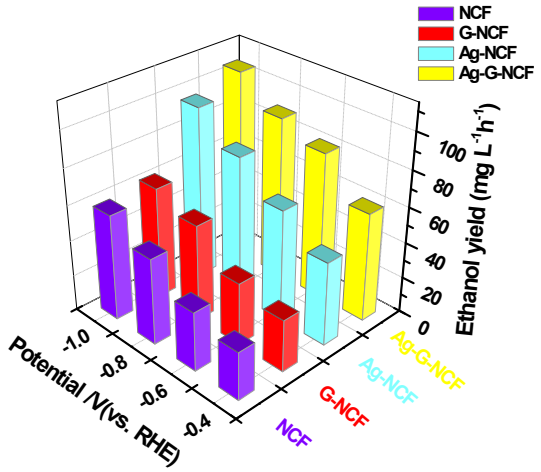

Figure S7. Yields of ethanol on NCF, G-NCF and Ag-NCF and Ag-G-NCF electrodes obtained from electrochemical reduction of CO_2 for 2h.

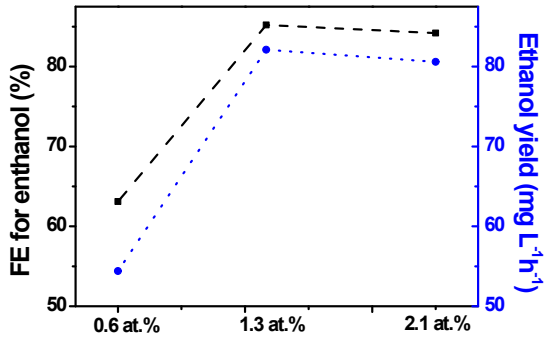

Figure S8. Faradic efficiency and yields of ethanol on Ag-G-NCF electrode with Ag contents of 0.6 at.%, 1.3 at.% and 2.1 at.% obtained from electrochemical reduction of CO_2 for 2h (-0.6 V).

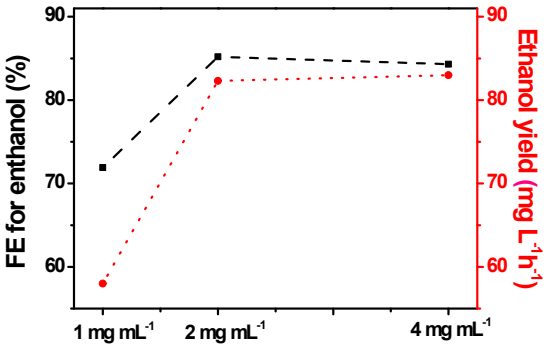

Figure S9. Faradic efficiency and yields of ethanol on Ag-G-NCF electrode with GO concentrations of 1 mg mL^{-1}, 2 mg mL^{-1} and 4 mg mL^{-1} obtained from electrochemical reduction of CO_2 for 2h (-0.6 V).

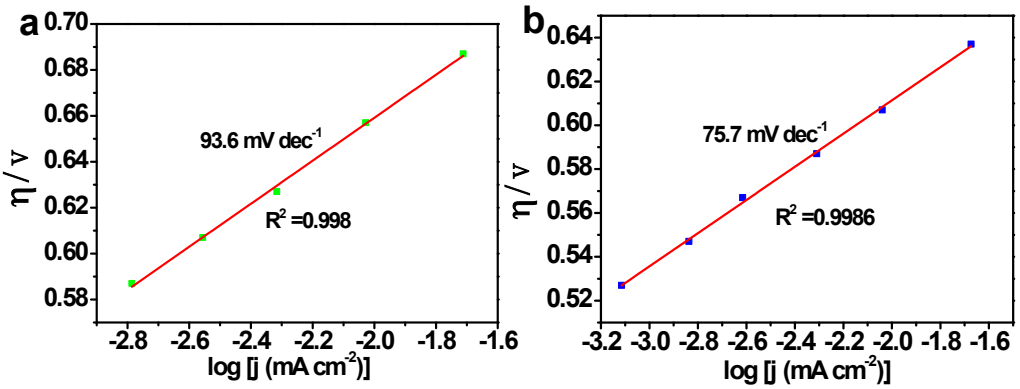

Figure S10. Tafel plots for CH_3CH_2OH production at (a) G-NCF and (b) Ag-G-NCF electrode.

NMR Identification and Quantification of Liquid Products

665 μL of catholyte was syringed out from cathode chamber cell after 120 min of the electrolysis. It was then mixed with 70 μL internal standard which was consisted of 25 mM phenol (99.5%, Scharlau) and 5 mM dimethyl sulfoxide (DMSO, 99.9%, Analytical pure reagents) in D_2O solution. 735 μL of this mixed solution was transferred to a NMR sample tube. Liquid products were quantitative analyzed by ^1H NMR (Bruker AV-400), and the water suppression method was used. The concentration of liquid products was determined by the standard curves drew from various known liquid (ethanol or formic) concentrations. Because the ratio of the peak area could reflect the ratio of concentration, the relative peak area can be calculated as follows:

$$Relative\ peak\ area\ ratio\ (ethanol) = \frac{Triplet\ peak\ area\ at\ 1.1\ ppm\ (ethanol)}{Singlet\ peak\ area\ at\ 2.6\ ppm\ (DMSO)}$$

$$Relative\ peak\ area\ ratio\ (formate) = \frac{Singlet\ peak\ area\ at\ 8.3\ ppm\ (formate)}{Triplet\ peak\ area\ at\ 7.3\ ppm\ (phenol)}$$

The concentration of these two liquid products was obtained using the calibration curves shown in Figure S11.

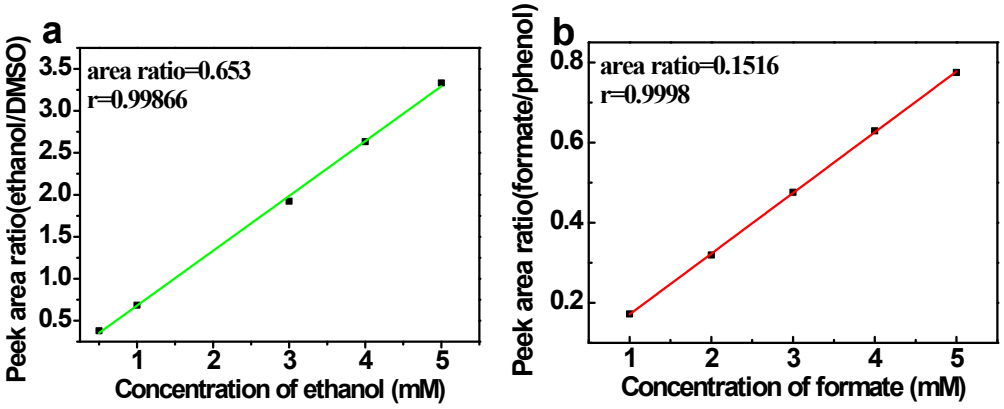

Figure S11. (a) Calibration curves for ethanol (left side, DMSO as internal standard) and (b) formate

(right side, phenol as internal standard).

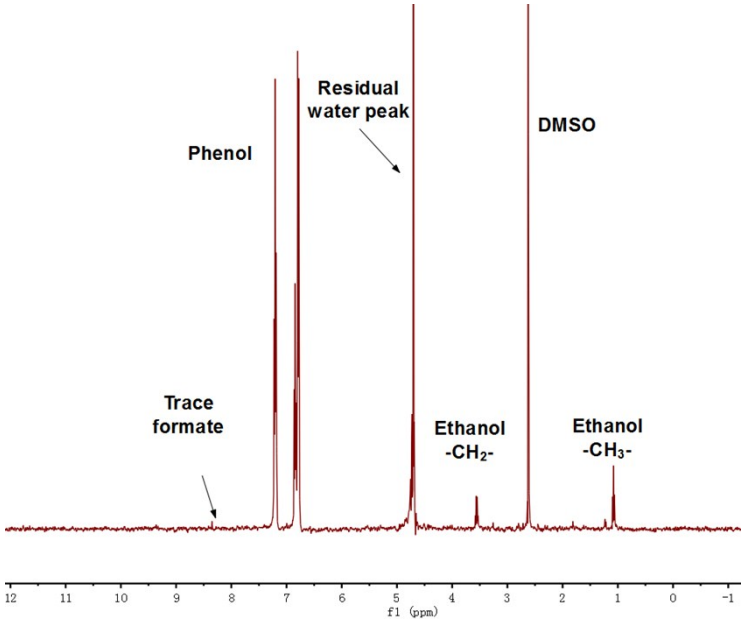

Figure S12. The ^{1}HNMR spectrum of the $KHCO_3$ catholyte after 2 h reduction on Ag-G-NCF. Potential applied = -0.6 V (vs RHE).

Method and Modeling

The kinetic energy cutoff for plane wave expansion was set at 450 eV, which is enough for two-dimensional layered graphene we just used. To avoid slab's interaction with their periodic images, a vacuum of 20 Å is used along the direction perpendicular to the layer. A Monkhorst-Pack mesh of 6×6×2 is used for integration in reciprocal space. The calculations were performed with a 5×5×1 supercell for N-doped graphene, 3×3×2 supercell for argentum partical. To obtain the optimized structures, the forces on all atoms were minimized to be smaller than 0.01 eV/Å.

Table S2. The bond length and binding energy of different adsorption sites (single-pyridinic N, triple-pyridinic N, triple- pyrrolic N)

	Bond length (Å)	Binding energy (eV)
single-pyridinic N	1.01	1.29
triple-pyridinic N	1.58	2.42
triple- pyrrolic N	0.94	1.38

Table S3. The bond length and binding energy of different adsorption sites (Top site of argentum

surfaces, hollow site of argentum surfaces, bridge site of argentum surfaces)

	Bond length (Å)	Binding energy (eV)
Top site of argentum surfaces	2.12	0.27
Hollow site of argentum surfaces	2.25	0.15
Bridge site of argentum surfaces	2.49	0.24